

## **1. IDENTIFICATION AND SIGNIFICANCE OF THE PROBLEM OR OPPORTUNITY**

The development of increasingly more complex and integrated aerospace vehicles that are capable of a variety of missions is leading engineers and scientists to consider nonconventional airframes, new structural and propulsion concepts and their interactions early in the design cycle. This greater range of design options must be examined in cross disciplinary terms, where individual disciplines are allowed to challenge the constraints of other disciplines. Cross disciplinary design space exploration is needed to reduce uncertainty and increase knowledge in order to make better decisions. The large dimensionality of such a design space requires the use of low-fidelity methods at the conceptual design stage, but the overarching goal is to construct a broad, yet detailed and accurate picture of the design space. Therefore, there is also a need to incorporate high-fidelity analysis tools early in the design process. Mixed fidelity models are an enabling technology, allowing the design of individual system components to be understood within the broader context of a full system. Increased computational power and the proliferation of new unmanned aerial vehicle designs have been driving forces in the development of a number of variable fidelity software systems and frameworks over the last decade. Yet, a number of fundamental issues in multifidelity computing remain unresolved. This proposal seeks to pioneer innovative methods for managing data on various levels of fidelity through extensions of previous methods, computational results, and rigorous mathematical results. Specifically, Multifidelity Sequential Kriging Optimization (MFSKO) will be extended to address multi-criteria optimization involving more than a single type of model representing more than a single discipline. Also, rigorous convergence results from Schonlau (1997) will be extended to multifidelity optimization in the context of radial basis function methods and Kriging models. Adaptive methods will be developed to achieve probabilistic convergence results and enhance performance. Results will be illustrated using a flying wing UAV design function integrating information from structural and fluid models.

Advanced aerospace vehicle design methods must fuse data from multiple sources and various levels of fidelity. In a multifidelity framework, the resolution and fidelity of simulations should be tailored to the requirements of the analysis. There are many factors to consider, including the spatial resolution, temporal resolution, physical processes being modeled, the number of objects, number of attributes of each object, and the degree of interaction between these objects (Gardner and Hennigan, 2003).

High-fidelity methods are typically more expensive, and must be used sparingly out of practical necessity. Other factors to consider are that high-fidelity analyses are assumed to be more accurate, but may not always be, and that there are often difficulties related to obtaining good gradients. For example, integer/discrete variables associated with gross topological changes, e.g., number of compressor stages, number of engines, control surfaces and so on, amount to major discontinuities (“cliff edges,” in Jarrett’s (2006) terminology) which computationally efficient gradient-based design optimization methods cannot cross.

An obvious advantage of low-fidelity methods is that they are cheap and fast. More rarely mentioned are the potential benefits of low-fidelity methods in a multifidelity framework, namely that they enable effective design exploration, not merely because of their speed, but as an aid to escape noisy local optima due to the nonsmooth nature of the design space, a common occurrence in the case in high-fidelity analyses. Low-fidelity methods enable safe transit between local optima, effectively tunneling back and forth through the cliff edges that discrete variable problems bring about (Jarrett, 2006). The disadvantages of low-fidelity tools are that they may produce inaccurate results. Also, low-fidelity tools may not work for unconventional designs or strongly nonlinear regimes (Wintzer et al., 2006), or may not be able to produce the quantities of interest (e.g. aerodynamic drag).

A significant issue in multidisciplinary frameworks is the difficulty in specifying consistency between models. A low-fidelity and high-fidelity model are said to be *weakly consistent* if “the projection of the state of the higher resolution model to the space of the lower resolution model is sufficiently close to the state of the low resolution model” (Gardner and Hennigan, 2003). In many applications, lower fidelity refers to lower resolution, but also different methodologies altogether involving significant approximations, not only missing detail but also missing physics (e.g., absence of chemical reactions, aeroelastic/unsteady effects, viscosity, or turbulence). In such cases, one cannot guarantee even *weak consistency*.

This proposal addresses some of the questions lying at the heart of multifidelity computing (whether modeling, optimization, or design). True integration of the results from codes of varying fidelity poses a number of challenges. One of them is the fact that prediction codes of varying fidelity levels use different input parameterizations and, therefore, operate in different spaces (Robinson et al. 2006a,b). Another challenge is the development of effective strategies when low- and high-fidelity models are not consistent, or when weak consistency is satisfied only in a small region of the design space, therefore limiting the efficiency of current multifidelity frameworks and, potentially, the breadth of design options being considered. The question of optimal sampling of the design space given limited resources is a critical one that is fundamentally linked to the characterization of uncertainty and uncertainty requirements. Specifically, there is a need to develop rigorous approaches addressing not only where to sample the design space, but also at what level of fidelity. These questions are key to a successful and comprehensive multifidelity system.

Alexandrov et al. (2000) demonstrated an Approximation Management Framework for solving optimization problems using variable fidelity models. In this approach, low-fidelity predictions are modified using a “correction technique” due to Chang et al. (1993) and formalized into a trust region management framework. The advantage of this type of approach is that it is provably first-order convergent to the high-fidelity optimum. As pointed out by Alexandrov et al., the low-fidelity approximation does not need to be a good approximator of the high-fidelity model, as long as it has suitable predictive properties for the purposes of optimization. In the worst case scenario where the low-fidelity and high-fidelity predictions and trends contradict each other, the approach simply reverts to conventional optimization using the high-fidelity model. Predictably, the method is most beneficial when a favorable relationship between low and high fidelity is maintained over a sizable portion of the design space.

In the past decade, there have been numerous implementations of variable fidelity ideas based on this concept of “bridge functions” as a re-anchoring framework to correct low-fidelity analyses to approximate the results of high-fidelity analyses. The “beta” factor initially proposed by Chang is introduced as a local multiplicative factor, although many researchers (e.g., Hatanaka et al., 2006, Ghoreyshi et al., 2008) have found it advantageous to implement the additive form of the correction, perhaps because of the difficulties associated with getting good gradients in high-fidelity analyses. Many of the current approaches are based on local correction response surface-type ideas which are locally valid. These schemes incorporate Taylor expansion-based corrections between the low- and high-fidelity models. These correction schemes work if the design space is smooth. The corrections are local in nature. Often they are implemented as either additive or multiplicative-type corrections and require that both low- and high-fidelity data be available at the same point. These factors tend to result in relatively frequent high-fidelity updates and, therefore, only modest improvements in computational savings over conventional optimization. By contrast, the performance advantages alone of a method allowing bold steps across the design space can produce significant net computational savings (Reisenthel and Lesieutre, 2007).

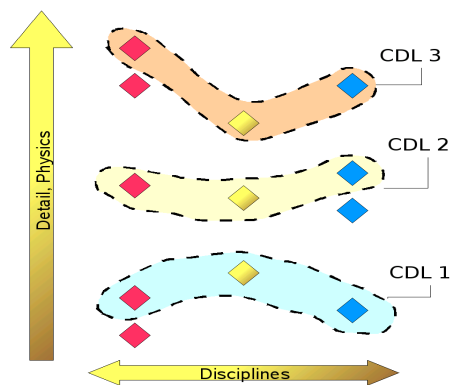


**Figure 1.** Analysis Tools, Ranked by Fidelity, Organized by Discipline, are Linked in Cross Disciplinary Groups.

It is NEAR's assertion that the approach of correcting a low-fidelity model and updating it in some trust region is neither fully integrated nor global and that, in turn, this approach could prove overly conservative. While useful for establishing provable convergence to high-fidelity results/optimization, the local correction method has a tendency to limit the step sizes taken in optimization and, more generally, curtails the size of the design space exploration. By contrast, an approach that exploits the results of bold steps so as to cumulatively update a variable fidelity metamodel may be more beneficial, especially in the early stages of a high-dimensional cross disciplinary design.

A summary of the proposed innovation is given in the notational plots of **Figures 1-3**. **Figure 1** depicts a “map” of analysis codes spanning three hypothetical disciplines, e.g., fluids, structures, and guidance and control. Each analysis code is represented by a  $\diamond$  symbol and is ranked vertically according to its level of fidelity, representing both the level of the physics included in the

model and the level of geometric detail being modeled. Within a multidisciplinary multifidelity framework, codes with compatible fidelity levels are first coupled together using cross disciplinary links (CDL). Such groupings are the staple of multidisciplinary optimization (MDO). Within each group, not only are variables appropriately exchanged between disciplines, but the processes for information exchange/update are well-defined. For example, the disciplines within a group can be tightly integrated or loosely coupled, physical interactions accounted for explicitly or through subiterations between codes, and so on. In addition, optimization schemes within a group can include a wide array of methods, ranging from collaborative optimization (Braun et al., 1996) and multidisciplinary optimization under uncertainty (Sun et al., 2006), to reliability-based (Mourelatos et al., 2005) and risk-based design optimization (Reisenthel and Lesieutre, 2007). This proposal recognizes that, while multidisciplinary analysis (MDA) may not be considered a “mature science,” it is a well-developed one. The innovation described here focuses primarily on the multifidelity aspects of aerospace vehicle analysis and design. Thus, the “isofidelity”-groupings depicted in **Figure 1** represent an encapsulation of analysis tools, solution methods, and information exchange processes which can operate independently of each other. The question raised here is how to merge and manage the information from these multiple fidelity groupings.

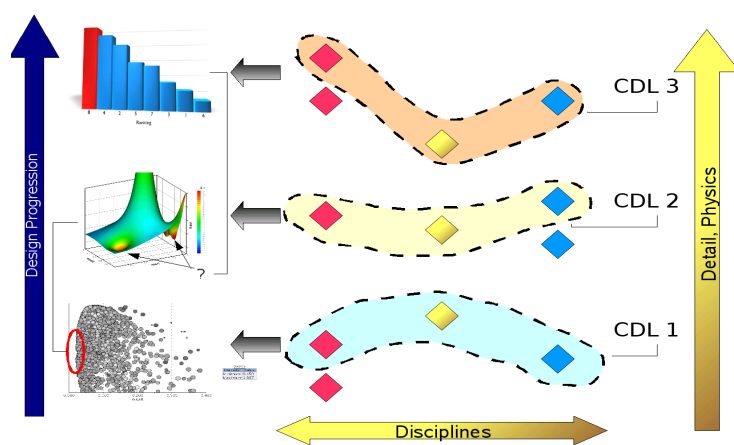


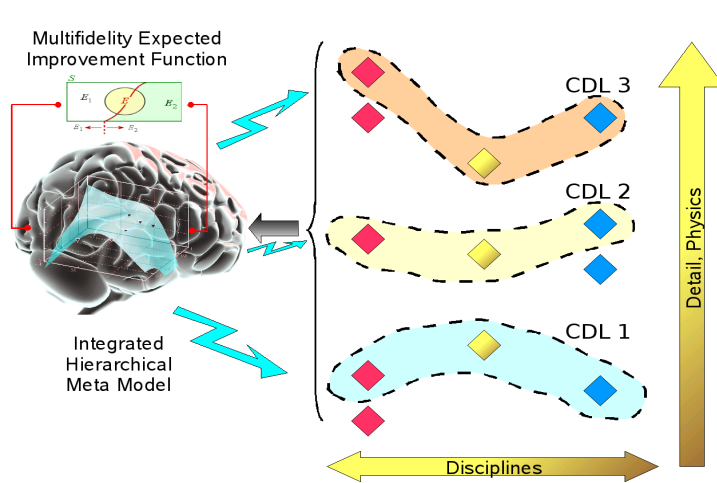
**Figure 2.** Conventional View of the Design Process over Time.

**Figure 2** depicts a conventional view of the design process as decisions evolve over time. In the conceptual design stage and, increasingly, in preliminary design a large array of options and cross disciplinary trades are considered, even though the knowledge of the system is necessarily imprecise (Lewis and Mistree, 1998). This is traditionally the *design space exploration* phase, where individual disciplines must be able to challenge the constraints of other disciplines (Holden and Keane, 2004) in order to come up with effective solutions. An outcome of these analyses (CDL 1 in **Figure 2**) is, typically, to narrow down the design space to smaller, more

manageable portions which are subsequently investigated in more detail. The intermediate level of fidelity (CDL 2), though more expensive, is then used to refine the analysis, add geometric detail, and increase the physical fidelity of the models used, thus reducing the uncertainty in the design. Cross discipline interactions are retained in the MDO methods used, but a smaller portion of the design space is considered, in order to make this tractable in spite of the higher costs. Finally, the detailed design stage (CDL 3) is used to further refine the analysis, focusing the design to a handful of options. These options and their immediate vicinity are investigated using the highest fidelity methods that can be afforded, further reducing the uncertainty, and eventually resulting in a ranking of the solutions and decision making. As previously mentioned, this *decoupling* of the different fidelity levels, except from a design history point of view and for the purpose of narrowing the design, has several drawbacks: (a) it takes a long time, (b) it is not an integrated model and, thus, does not benefit from cumulative mutual data set enrichment, (c) it does not truly address when high, medium, and low fidelity are appropriate, except in the limited, pre-ordained sense discussed above, and (d) it is a one-way street, in the sense that it is not conducive to revisiting other areas of the design space as the project matures and uncertainty decreases. This last point is particularly important, in terms of sampling strategy in global optimization systems (Reisenthel et al., 2007). While a strategy that primarily emphasizes exploration is a waste of computational resources, it is also evident that one based on exploitation represents a loss of design opportunity since it is conditioned by the initial seeding of the design space, and is destined to end with the first promising region found. The ideas of Jones et al. (1998) and Sóbester et al. (2005) which call for a proper balance of exploration and exploitation, are most attractive in this regard and provide a rational framework for the allocation of computational resources.

By contrast with the conventional view, the proposed multifidelity multidisciplinary framework (**Figure 3**) is a true *integrated* hierarchical model which takes into account (merges) the information from multiple fidelity levels and manages this information in order to achieve optimal sampling of the design space, both

in terms of design variables and level of fidelity (see Section 3). The two key innovations are as follows. The first innovation is the merging of all multifidelity data into a probabilistic response surface-based metamodel. This “Integrated Hierarchical Metamodel” will build on the foundation provided by data fusion methods (Reisenthel et al., 2006) and optimization methods (Reisenthel and Lesieutre, 2007) using probabilistic radial basis function (RBF) networks. The second key innovation (labeled “Multifidelity



Expected Improvement Function” in **Figure 3**) will enable the management of when high-, medium-, and low-fidelity analysis tools are appropriate as the “next move” in design space exploration/exploitation and metamodel update. The goal of balancing exploration and exploitation in a mathematically rigorous way will be achieved by using an integrated criterion to determine both the location and fidelity level of subsequent searches and will be based on Kennedy and O’Hagan’s (2000) original work in the UK, and subsequent refinements by NEAR’s Research Institution STTR partner, Prof. Allen and his coworkers at OSU (Huang et al., 2006, Schenk et al., 2005).

**Figure 3.** Integrated Hierarchical Framework.

The proposed hierarchical integrated methodology will be cumulative, metamodel-based, and will incorporate key enhancements in multifidelity space exploration sampling strategy. The gappy Proper Orthogonal Decomposition (Robinson et al., 2006) will be used for dealing with multifidelity models with different input variables. Details on the core hierarchical metamodeling effort, its proposed enhancements, and their combined application to the aerostructural design of a simplified UAV are given in the Work Plan section.

## 2. PHASE I TECHNICAL OBJECTIVES

The broad objective of this work is to pioneer innovative methods for representing, managing, and fusing information of various levels of fidelity within an engineering discipline and across multiple disciplines for a wide-range of analysis and design tools. Research questions to be answered in this effort are as follows:

- What are the benefits of a hierarchical integrated global metamodel for multifidelity data?
- Can Huang’s multifidelity design space sampling strategy be extended to manage system updates within an integrated hierarchical global metamodeling approach?
- What are the trade-offs and limitations of MFSKO and RBF frameworks?
- How effective are global multifidelity models, relative to bridge functions, as a re-anchoring framework to correct low-fidelity data? What is the theoretical connection between these schemes?
- Can rigorous proofs of convergence to the high-fidelity optimum be developed?

A successful cross disciplinary demonstration of the proposed techniques will provide the foundation for cost-effective multifidelity design space exploration and management of advanced airframes.

## 3. WORK PLAN

The present section is organized as follows. We begin (Section 3.1) by summarizing the various innovations identified in Section 1. The result is a list of desirable attributes a multidisciplinary, multifidelity computing environment must have for the effective integration/design of advanced airframe concepts. It is then argued that these attributes can be built upon the foundation provided by the cumulatively enhanced global

metamodel framework, an embodiment of which is presented in Section 3.2. A list of the specific tasks to be carried out in Phase I is then presented in Section 3.3, including the definition of a baseline problem and the application of the proposed concepts to this baseline problem. This section is then concluded with the timetable for the proposed effort.

### 3.1 Innovation Summary

Among key ideas expressed in Part 1, Huang et al. (2006) used a modified version of Kennedy and O'Hagan's (2000) autoregressive model for multifidelity prediction in which a high-fidelity simulation is approximated by a lower fidelity simulation plus a delta term assumed to be independent of the previous predictions. Huang et al. (2006) successfully used kriging metamodels for the delta terms. A pilot study at Sandia (Swiler, 2006) implementing the Kennedy-Huang idea using Gaussian processes reached similarly promising conclusions. The focus of our attention, however, is a byproduct of this theory, namely the resulting multifidelity exploration sampling strategy proposed by Huang et al. One of the items of the Phase I work plan is to develop, implement, and test a modified version of Huang's integrated multifidelity expected improvement function as a comprehensive strategy for multifidelity data sampling. This strategy has proven successful in multifidelity optimization problems outside aerospace (Huang et al., 2006, Schenk et al., 2005). Most significantly, the algorithm takes into account both the location (in design space) *and* the fidelity of further data acquisition. Key elements of this concept will be adopted and implemented within the proposed cumulative metamodel concept. Detailed equations in support of the implementation are presented at the end of Section 3.2.

As will be seen in Section 3.2, the multifidelity cumulative metamodel concept relies formally on a straightforward dimensionality augmentation of the input data (control variables) space by including the fidelity level as an additional variable. Because the metamodel predictions are always projected on a given-fidelity subset (typically the highest fidelity), the number of operations or computational work in a design exploration study is no greater than the original number of control variables demands.

### 3.2 Cumulative Global Metamodel Framework

The present section provides some technical background and its application to multifidelity modeling, followed by a simple embodiment of the proposed cumulative global metamodel approach.

#### 3.2.1. Technical Background

The task of formulating an ordinary response surface in  $N$ -dimensional space amounts to identifying a smooth mapping  $F : \mathbb{R}^N \rightarrow \mathbb{R}$  on the basis of  $p$  available data points. If this response surface acts as an interpolant, then the function  $F$  must satisfy the constraints  $F(X_i) = Y_i$ ,  $i = 1, \dots, p$  where each  $X_i$  is a vector of independent variables (for example, spatial coordinates, flow conditions, design variables), and each  $Y_i$  is a dependent variable (for example, pressure). In the case where  $F$  represents a *fit* to the data, then the response surface is required to minimize the distance  $\|F(X_i) - Y_i\|$ , typically in the least squares sense. This goal can be achieved by a number of different means including kriging, multivariate adaptive splines, and Support Vector Machine (SVM) algorithms. The present approach uses a radial basis function (RBF) network to represent the function  $F$ . In this approach,  $F$  is expanded into basis functions  $\phi_k$  which are radially symmetric about their control point,  $\chi_k$ . By analogy with SVMs, we refer to  $(\chi_k; F(\chi_k))$  as the *support vectors* for the response surface. Thus,

$$F(X) = \sum_k c_k \phi_k(X), \quad \phi_k(X) = f(\|X - \chi_k\|; b) \quad (1)$$

where  $f$  is a scalar shape function,  $b$  is an adjustable scale or stiffness parameter, and  $\|\cdot\|$  designates the Euclidean norm. The  $c_k$  are basis function coefficients, the solution to a least-squares linear problem

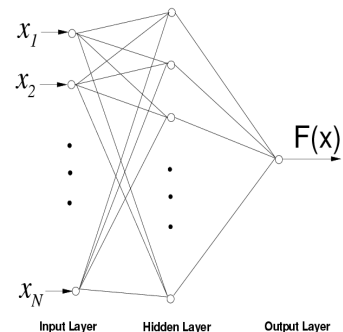


Figure 4. RBF Network.

in which each row is an instantiation of the constraints  $F(X_i)=Y_i$ . Radial basis function models can be viewed as a three-layer feedforward neural network with linear output mapping. This is shown schematically in **Figure 4**, where the number of nodes in the hidden layer is equal to the number of basis functions, the inputs  $x_i$  are the coordinates of  $X$ , and the weights of the output layer are the coefficients  $c_k$ . Also, the shape function ( $f$ ) is the activation function of the hidden layer nodes, which can take a number of forms, e.g., Gaussian, thin plate spline, multiquadric, or reciprocal multiquadric.

There are, *a priori*, a number of different ways of selecting the control points  $x_k$ . One possible approach is the use of sequential approximation and optimization methods. This can be quite expensive, and a more efficient approach to control point selection consists of using a fixed subset of the existing training data. Algorithms such as generalized cross-validation (GCV) can be used for this purpose, resulting in parsimonious networks with good generalization properties. While the use of a small number of regressors  $\phi_k$  is indeed desirable from the point of view of model robustness, we will confine the present discussion to simple networks where the training data are assumed deterministic and sparse. Thus, in this particular implementation, the number of basis functions is equal to the number of training data points, and the centers (control points  $\xi_k$ ) of the RBFs coincide with the data points. As a result of this simplification, there is no need for stepwise regression algorithms: the structure of the equivalent neural network (**Figure 4**) is automatically determined by the data.

One important addition to these ideas is the concept of response surface uncertainty. In the following, it is shown that, due to linearity-in-the-parameters, it is possible to make use of well-established statistical results to propagate the uncertainty of the support data onto an uncertainty of the response surface itself.

Consider the original equation  $[A][C]=[Y]$  as a regressor model for the data, i.e.,  $[A][C]=[Y]+[e]$  where  $[e]$  is the modeling error. Let  $[A]=[Q_1][\Sigma][Q_2^T]$  designate the singular value decomposition of the matrix  $[A]$ . The pseudoinverse solution is then given by  $[\hat{C}] = ([Q_2][\Sigma^+][Q_1^T])[Y]$ . It can then be shown, under certain simplifying assumptions, that the covariance matrix of the solution vector is

$$cov[C] \equiv E[(\hat{C}-C)(\hat{C}-C)^T] = \sigma^2 E[Q_2 \Sigma^+ \Sigma Q_2^T] \quad (2)$$

where  $E[\cdot]$  designates the expected value, and  $\sigma^2$  is the variance, presumed uniform, of  $[e]$ . Equation (2) propagates the “measurement” uncertainty in  $[Y]$  onto the solution vector  $[C]$ . The matrix  $[Q_2 \Sigma^+ \Sigma Q_2^T]$  can be interpreted as redistributing the measurement noise onto the solution vector components. It then follows that

$$E[(\hat{F}-F)^2] = \sum_i \sum_j (cov[C])_{ij} \phi_i(X) \phi_j(X) \quad (3)$$

Equation (3) represents the variance  $var(F)$  of the response surface. Assume a Gaussian probability distribution. The resulting uncertainty on  $F(X)$ , defined as  $\Delta F = \pm 3 \sqrt{var(F)}$  (“three-sigma” uncertainty), is shown in the hypothetical example of **Figure 5**. The dependent variable uncertainty of the training data is indicated in the form of vertical error bars. The resulting uncertainty on the response surface is indicated in the form of upper and lower bounds,  $F \pm \Delta F$ , using thin dashed lines.

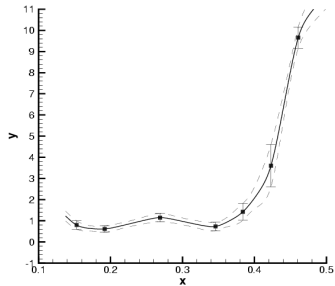


**Figure 5.** Response Surface +/- Uncertainty.

Note that, in order to propagate uncertainty according to the method described above, the variable  $[e]$  must be a stochastic variable such that  $cov[e] = \sigma^2[I]$  where  $[I]$  is the identity matrix. In other words,  $[e]$  must have zero cross-correlation, and must be of uniform variance  $\sigma^2$  across all of its components. While the zero cross-correlation assumption is typically not justified if there is a deterministic bias between the regressor model and the data, it is practical to use the above equations to propagate uncertainty, by assuming  $[e]$  represents a vector of random measurement errors  $[\delta Y_1, \delta Y_2, \dots, \delta Y_p]^T$ . When these

seed uncertainty levels differ from support vector to support vector, such as in the example of **Figure 5**, then both left- and right-hand sides of  $[A][C] = [Y]$  are multiplied by a weighting matrix  $[W]$ , where  $[W]$  is defined in tensor notation as  $W_{ij} = \delta_{ij} / \sqrt{\text{var}(Y_i)}$ . This simple algorithm ensures that the variance of the transformed variables is uniform. In the above discussion, the uncertainties are assumed to be uncorrelated between data points. If this were not the case, then more sophisticated techniques, such as Markov estimators and/or instrumental variables can be used.

### 3.2.2 Application to variable fidelity modeling

Consider the general notion (Li et al. 1993) of data fusion defined as “the combination of a group of inputs with the objective of producing a single output of greater quality and reliability.” For the purposes of this example, assume the existence of two data sources representing the results of low- and high-fidelity simulations respectively, although the methodology presented here is easily extended to multiple fidelity levels. The premise is that simultaneous consideration and integration of these multiple data sources (fidelity levels) enhances global data understanding. We will confine the analysis to the case of low- and high-fidelity data. Specifically, we focus on the situation where the low-fidelity data are reasonably affordable to obtain, in contrast to the high-fidelity data, which are assumed to result from expensive simulations at a limited number of configurations and flow conditions. Note that the high-fidelity and low-fidelity data need not be sampled at the same conditions. We assume the typical situation where the high-fidelity data are sparse, with respect to the low-fidelity data.

The basic idea behind the use of response surface technology for integrated modeling of high-fidelity and low-fidelity data is to take advantage of the radial symmetry of the basis functions to construct a metamodel that incorporates all fidelity levels simultaneously. In the present example, this can be done by adding an auxiliary variable  $\varepsilon \equiv x_{N+1}$  to the multidimensional design space  $(x_1, x_2, \dots, x_N)$ . This extra variable is binary in nature, and is used to tag whether the data are low-fidelity ( $\varepsilon = 0$ ) or high-fidelity ( $\varepsilon = 1$ ).

A single global response surface is then calculated in  $N+1$  dimensions. By querying the response surface projection along  $\varepsilon = 1$  one obtains a model representation which respects the integrity of the high-fidelity data, while simultaneously “inheriting” key features of the supporting low-fidelity model. To visualize how the method works, consider the sketch shown in **Figure 6**. The schematic lays out the position of the high-fidelity and low-fidelity support vectors relative to each other. The horizontal coordinate “X” symbolizes the independent variables  $(x_1, x_2, \dots, x_N)$ , i.e., the original design variables of the problem. The vertical coordinate represents the auxiliary variable  $\varepsilon$  or direction  $x_{N+1}$ .

The large circles around each point symbolize the region of influence or spatial correlation associated with each radial basis function. The radius of these circles is related to the scale parameter  $b$  in Equation (1). Thus, wherever the data sampling is high, the interpolant will be mostly influenced by the basis functions whose centers are in the immediate vicinity. On the other hand, when the high-fidelity data points are widely separated relative to the width of the basis functions, the interpolation will be affected primarily by the low-fidelity points. The evaluation of the global response surface in the high-fidelity plane (i.e., projected onto  $\varepsilon = 1$ ) has the effect of interpolating the high-fidelity data in a way that is rooted not in mathematics or simple-minded smoothness assumptions, but, rather, in whatever *physics* are contained in the low-fidelity model.

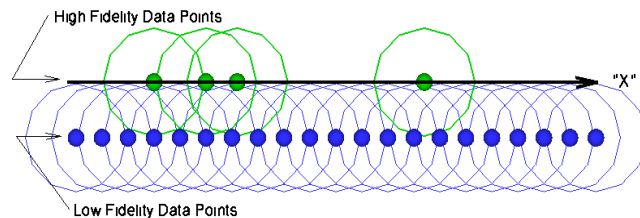


**Figure 6.** Low- and High-Fidelity Support Vectors Layout.

### 3.2.3 A One-Dimensional Example

To help better understand how this method works, consider the following missile aerodynamics application. In this one-dimensional example the high-fidelity data are not the results of simulations but of a wind tunnel test, although this does not change in any way the principle of operation. This application

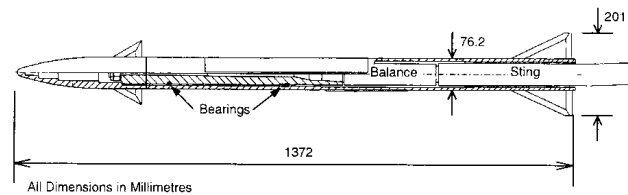


**Figure 7.** Details of Wind Tunnel Model (reproduced from McIlwain et al., 1998 with permission).

has the benefit of abundant high-fidelity data, thus allowing the illustration of the method using different data samplings. For reference, the high-fidelity data are from a series of wind tunnel tests carried out by Shorts Missile Systems Ltd. in the 1990s (McIlwain et al., 1998) for a free rolling missile body with a decoupled canard-controlled nose section (see **Figure 7**).

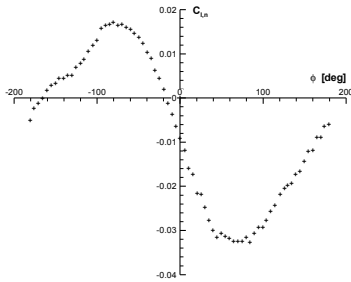


**Figure 8.** Nose Rolling Moment as a Function of Roll Angle. (Digitized from McIlwain et al., 1998, with permission).

**Figure 8** shows the static rolling moment  $C_{l,n}$  measured on the nose, as a function of the roll angle  $\phi$  at a freestream Mach number  $M = 3.5$ , total incidence angle  $\alpha_c = 8 \text{ deg}$ , and canard fins canted at 8 and 12 degrees (leading edge up) for the port and starboard fins, respectively. The high-fidelity data shown in **Figure 8** were taken at static conditions in order to compare them to CFD predictions. This configuration happens to present an interesting case where, at certain roll angles, the upper canard experiences partial shielding from the windward flow, due to the expansion over the nose, an effect which was correctly predicted by the CFD calculations (McIlwain et al., 1998). In this exercise, we repeat these CFD calculations with a finer roll angle increment, in

order to better capture the nonlinearities in the rolling moment variation. For multifidelity comparison purposes, a lower fidelity method which does not incorporate all of the proper physics is also used. The results of both methods are described next.

We begin with the use of the lowest fidelity computational data, not with the intent of showing what happens when one attempts to combine high-fidelity data with computations of inadequate fidelity, but simply as a more visually interesting case, since the trends between low- and high-fidelity data are unfavorable, and as a teaching tool for how the method works.

**Figure 9** illustrates the results of the process when augmenting the low-fidelity data with various sparsely sampled subsets of the high-fidelity data. Each plot in the figure portrays three entities: (1) the input data, i.e., both low-fidelity computational (dashed line) and high-fidelity experimental (red dots),

(2) the high-fidelity projection of the global metamodel output (solid green line), and (3) the complete set of wind-tunnel measurements (“+” symbols), representing the “truth” data. It must be stressed that only the input data are used in the global metamodel calculation. The validation data (“+” symbols) are presented for comparison purposes only, i.e., as a reference against which to judge the quality of the prediction. The inadequacy of the low-fidelity computational model taken by itself is evident. The forming of an integrated hierarchical metamodel using a single high-fidelity data point ( $\phi = 0 \text{ deg}$ ) together with the low fidelity is shown in the upper left graph of **Figure 9**. As expected, the hierarchical model produces a slight shift in the prediction in order to accommodate the new knowledge which the high-fidelity support vector represents. Let us now assume that a second high-fidelity data point is acquired at  $\phi \approx -135 \text{ deg}$  (upper right graph). The hierarchical model prediction at negative roll angles is now tilted upward. The prediction maintains the overall character of the low-fidelity computation, but it has “learned”

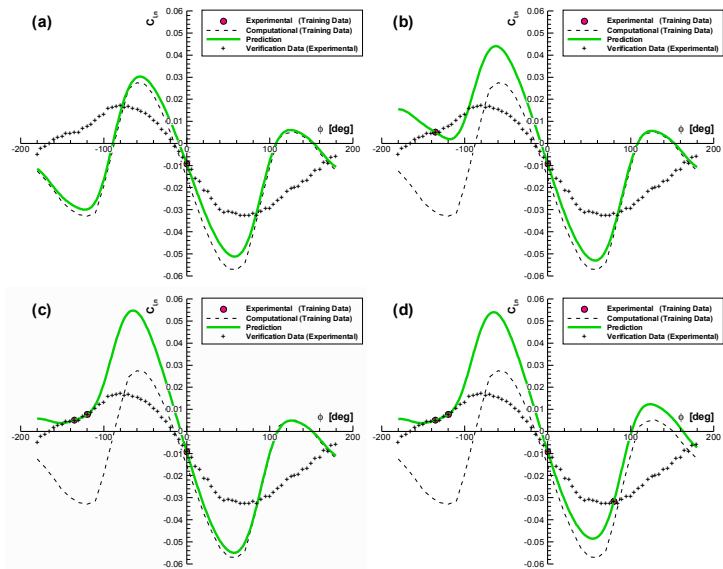


**Figure 9.** Integrated Hierarchical Model Predictions Using One (upper left), Two (upper right), Three (lower left), and Four (lower right) High-Fidelity Data Points.

from the significant high-fidelity correction/improvement at  $\phi \approx -135 \text{ deg}$ . Suppose a third high-fidelity data point is added (lower left graph,  $\phi \approx -120 \text{ deg}$ ). The hierarchical model prediction locally adapts to reflect the new information, eliminating much of the undershoot in the  $-135 \text{ deg} \leq \phi \leq -100 \text{ deg}$  roll angle range. In the lower right graph of **Figure 9**, the hypothetical addition of a fourth high-fidelity data point at  $\phi \approx 80 \text{ deg}$  results in an upward tilt of the prediction to, once again, accommodate the new information.

As anticipated from the geometric interpretation of **Figure 6**, the response surface respects and adjusts to the high-fidelity support vectors, while otherwise maintaining the overall character of the low-fidelity computational tool, whether in interpolation or extrapolation mode. It is worth noting, however, that given a sufficient number of high-fidelity data constraints, the influence of the low-fidelity computational data source will eventually become insignificant. This has previously been demonstrated on this particular example: by using high-fidelity data every 20 degrees (not shown), the RMS difference between the hierarchical model prediction and the full high-fidelity data set reduces from  $1.7 \times 10^{-2}$  (with four points) to  $6.6 \times 10^{-4}$  (using 19 points). In other words, the integrated hierarchical metamodeling approach does not prevent overcoming the limitations of a poorly chosen low-fidelity computational model, given sufficient high-fidelity data. The main interest, however, concerns the case where the high-fidelity data are sparse, because this will inevitably be the case when the number of independent variables is large. What happens when one uses a computational model that contains more appropriate physics is shown next.

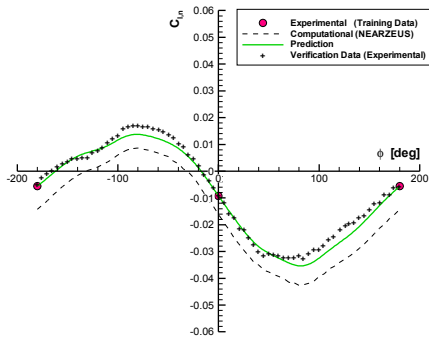


**Figure 10.** Integrated Hierarchical Metamodel Prediction Based on Euler CFD Prediction and Two High-Fidelity Data Points.

Instead of the lowest fidelity computational model used in **Figure 9**, the hierarchical metamodeling experiments depicted above can be repeated using a computational methodology of a more appropriate level (in this instance, an Euler CFD code). The Euler CFD data can be considered “medium fidelity” but formally assume the role of “low fidelity” data compared to the high-fidelity wind tunnel data. **Figure 10** depicts the integrated hierarchical metamodel prediction using as input data the “low-fidelity” Euler calculation results, augmented with only two high-fidelity data points at  $\phi = 0 \text{ deg}$  and  $\phi = \pm 180 \text{ deg}$ . The comparison between the integrated hierarchical metamodel prediction and the complete high-fidelity data set indicates a high degree of correlation. In particular, details of the aerodynamic nonlinearities predicted by the Euler methodology are visible in the projection response surface. With sparse high-fidelity data, the integrated hierarchical metamodel has been tailored to *learn* from the low-fidelity computational data, while

simultaneously adjusting to accommodate the available high-fidelity observations. Note that this particular implementation assumes the experimental data to be indeed of high fidelity, which is the rationale for evaluating the global response surface in the experimental “plane” ( $\epsilon = 1$ , see Section 3.2.2).

**Figure 10** corresponds to the nominal prediction  $F$  in Equation (1). It is worth mentioning that the variance on the prediction (not shown) is also automatically computed as a byproduct of this method.

As a final note of caution, the importance of performing the hierarchical metamodeling operations using a reasonable (weakly consistent) fidelity model is stressed in **Figure 11**, which compares the hierarchical metamodel predictions obtained by using the same two high-fidelity data constraints as in **Figure 10**, namely  $\phi = 0 \text{ deg}$  and  $\phi = \pm 180 \text{ deg}$ , but with low-fidelity data resulting from different analysis codes representing favorable

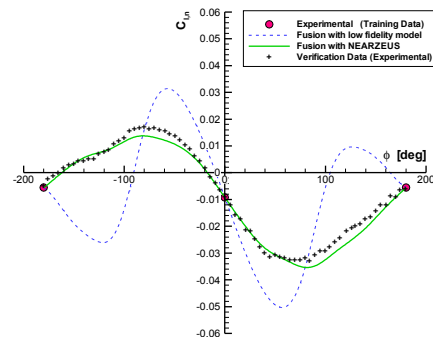


**Figure 11.** Comparison of Integrated Hierarchical Metamodel Predictions Based on Two Different low-fidelity Computational Data Sets.

and unfavorable conditions, respectively. The results shown in Figure 11 emphasize the importance of choosing low-fidelity models which incorporate the correct physics. This is especially true when performing sparse high-fidelity data interpolation, since the reliance on the low-fidelity data becomes greater. While the example of taking only two high-fidelity data points may appear extreme and somewhat academic, it is in reality highly relevant to the case of multidimensional data. When data are characterized by a large number of independent variables, finite resources (time and budget) impose limitations on the number of conditions that can be acquired. Modern design-of-experiment techniques can be used to maximize the amount of information that can be harvested from a given number of tests. But when the number of dimensions in the design space is large, “filling-in” the space in all variables remains a physical impossibility. Out of necessity, the data sampling will be sparse in at least some directions or regions of the parameter space. For another application involving three independent variables and sparse high-fidelity data, refer to Reisenel et al. (2006).

### 3.2.4 Multifidelity Design Space Management and Sampling Strategy

Kriging Modeling has been effectively used by researchers to model computer experiments which include finite element and finite difference methods (Sacks et al., 1989 and Schonlau, 1997). Sequential Kriging Optimization (SKO), also known as Efficient Global Optimization (EGO), was proposed by Jones et al. (1998) in the context of model computer experiments. The SKO method has its roots in the Bayesian Global Optimization method proposed by Kushner (1964). The EGO method was based on solving a curve fitting problem and another sub-optimization of the so-called “expected improvement” function maximization to determine where in the space the next functional evaluation should be executed. However, their treatment was restricted to cases with no random errors. Under these conditions, Schonlau (1997) proved that EGO will converge to the global minimum in a finite search space.

In work carried out by our STTR research institution partner, Prof. Allen and co-workers at OSU developed a multifidelity framework referred to as Multifidelity Sequential Kriging Optimization (MFSKO). Specifically, Huang et al. (2006a) extended the EGO method to cases with random errors and proposed an Augmented Expected Improvement function. Huang et al. (2006b) extended this method further to include data from varying sources such as experiments, simulations models, etc., to formulate Kriging models. This methodology called multifidelity modeling involves both the higher fidelity systems (actual system, e.g., experimental) and lower fidelity systems (simulation) for constructing the models. The term “fidelity” describes the accuracy with which these media can approximate systems of interest. Higher fidelity systems provide more accurate outputs than a lower fidelity one. However, the number of runs in a higher fidelity system is limited due to the high cost associated with the runs. Combining data from both higher fidelity and lower fidelity has the potential to reduce the cost while also providing a more accurate model.

As previously mentioned in Section 3.1, Huang et al. (2006) devised as a byproduct of their multiple fidelity sequential kriging optimization an integrated criterion to determine both the location *and* fidelity level of subsequent searches or evaluations. This criterion represents somewhat of a break with respect to conventional trust region management frameworks. It is fundamentally a *global* criterion. As such, it permits/can suggest bold exploratory moves across the design space, which is an approach that holds considerable promise for effective multidimensional and multifidelity space exploration. Huang et al.'s criterion is tightly integrated with their multiple fidelity kriging metamodeling approach, itself based on Kennedy and O'Hagan (2000). It assumes the existence of  $m$  different simulations to draw evaluations from, with the output functions ordered from lowest to highest fidelity  $f_1(\mathbf{x}), f_2(\mathbf{x}), \dots, f_m(\mathbf{x})$  where  $\mathbf{x}$  is the input vector. An autoregressive model linking these outputs is then postulated as follows:

$$f_k(\mathbf{x}) = f_{k-1}(\mathbf{x}) + \delta_k(\mathbf{x}), \quad (k = 2, 3, \dots, m) \quad ; \quad f_1(\mathbf{x}) = \delta_1(\mathbf{x}) \quad (4)$$

where the delta terms are all modeled by kriging. Because this method integrates data at all levels of fidelity to build a kriging metamodel as a global prediction, it is possible to use the associated Expected Improvement (*EI*) function as the criterion determining the location and fidelity level of subsequent evaluations (Schenk et al. 2005):

$$EI(\mathbf{x}, k) \stackrel{\text{def}}{=} E \left[ \max(\hat{f}_m(\mathbf{x}^*) - f_m^p(\mathbf{x}), 0) \right] \cdot \text{corr} \left[ f_k^p(\mathbf{x}), f_m^p(\mathbf{x}) \right] \cdot \left( 1 - \frac{\sigma_{\mu, k}}{\sqrt{s_k^2(\mathbf{x}) + \sigma_{\mu, k}^2}} \right) \cdot \frac{\text{Cost}_m}{\text{Cost}_k} \quad (5)$$

where  $f_m^p$  is the posterior distribution for  $f_m$ ,  $\hat{f}_m$  its best linear predictor, and  $\text{Cost}_1 < \text{Cost}_2 < \dots < \text{Cost}_m$  denote the cost per evaluation of each fidelity system  $1, \dots, m$ .  $\sigma_{\mu, k}^2$  is the unexplained variance of the

kriging model at level  $k$ , and  $s_k^2(\mathbf{x})$  is the variance of  $f_k^p(\mathbf{x})$ . The correlation term in Equation (5) is used to discount the expected improvement when an evaluation from a lower fidelity surrogate is used. The term involving  $\sigma_{\mu,k}^2$  accounts for diminishing returns of additional replicates as the prediction becomes more accurate, and the cost ratio adjusts the sampling strategy according to the evaluation costs (Huang et al. 2006). The location and fidelity of the next evaluation,  $\mathbf{x}_{n+1}$  and  $k_{n+1}$  are given by maximizing  $EI$ , i.e.:  $(\mathbf{x}_{n+1}, k_{n+1}) = \arg(\max(EI(\mathbf{x}, l)))$ . In Equation (5) the current effective best solution  $\mathbf{x}^*$  is defined by  $\mathbf{x}^* = \arg(\max(u(\mathbf{x})))$  where  $u(\mathbf{x}) = -\hat{f}_m(\mathbf{x}) - \mu s_m(\mathbf{x})$  expresses the willingness to trade one unit of the predicted objective for  $\mu$  units of the standard deviation of the prediction uncertainty (Schenk et al., 2005). Also, the expectation in Equation (5) is conditional given the past data and given estimates of the correlation parameters. Thus, the expectation is computed by integrating over the distribution of  $f_m^p(\mathbf{x})$ , with  $\hat{f}_m(\mathbf{x}^*)$  fixed. Based on results in Jones et al. (1998), the expectation can be calculated analytically as follows:

$$E\left[\max\left(\hat{f}_m(\mathbf{x}^*) - f_m^p(\mathbf{x}), 0\right)\right] = \left(\hat{f}_m(\mathbf{x}^*) - \hat{f}_m(\mathbf{x})\right)\Phi\left(\frac{\hat{f}_m(\mathbf{x}^*) - \hat{f}_m(\mathbf{x})}{s_m(\mathbf{x})}\right) + s_m(\mathbf{x})\phi\left(\frac{\hat{f}_m(\mathbf{x}^*) - \hat{f}_m(\mathbf{x})}{s_m(\mathbf{x})}\right) \quad (6)$$

where  $\Phi$  and  $\phi$  are the standard normal probability density and cumulative distribution functions, respectively. The expected improvement function defined above in the context of kriging models involves maximizing greedily the expected value of improvement of the objective from a single additional iteration followed by termination. Because of the noise potentially in all past data, the formulation is only approximate because one does not know the best solution. Instead, at every iteration the algorithm only has the effective best solution,  $\mathbf{x}^*$  defined above.

One aspect of the proposed work will be to implement the MFSKO within NEAR's integrated meta framework with the possibility in Phase II of extending MFSKO to address mixed continuous/integer optimization problems of the type that frequently occur in the conceptual and early stages of design. While there is tangible evidence (Huang et al., 2006, Schenk et al., 2005) that the MFSKO approach holds significant promise for aerospace design problems, it is desirable to place the proposed methods on a solid mathematical foundation going forward. Therefore, a second aspect of this work will be to extend the rigorous convergence results from Schonlau (1997) to multifidelity optimization in the context of radial basis function (RBF) and kriging models. It should be possible to develop a structure that is equivalent to the computational steps of Equations (4) and (5) for the case of integrated RBF-based hierarchical global metamodels since these share common properties with kriging. For example, we anticipate that key elements of Huang et al.'s multifidelity expected improvement function (Equation (5)) can be adapted with rigor to the proposed cumulative metamodeling concept. Referring back to the notation used in the Technical Background, this is likely to result in a formulation in which  $f_k^p(\mathbf{x})$  is replaced by  $F^{new}(x_1, x_2, \dots, x_N, \epsilon_k)$ ,  $\hat{f}_m(\mathbf{x}^*)$  is replaced by  $F^{pred}(x_1^*, x_2^*, \dots, x_N^*, \epsilon_m)$ , and  $var(F(x_1, x_2, \dots, x_N, \epsilon_k))$  is substituted for  $\sigma_{\mu,k}^2$ . Careful analysis and testing will be required to formulate a principled approach, however, and this will be part of the Phase I work.

In addition to extending rigorous convergence results from Schonlau (1997) to multifidelity optimization in the context of radial basis function methods and Kriging models, adaptive methods will be developed to achieve probabilistic convergence results and enhance performance. Results will be illustrated using the aerostructural design of a flying wing (X-47 UCAV-type) UAV.

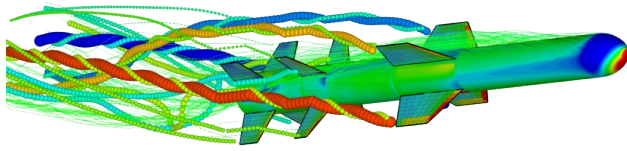
### 3.2.5 Definition of Baseline Problem

A baseline problem will be defined on which to develop and demonstrate the candidate (RBF and MFSKO) approaches for representing and integrating information from each discipline and model. Computational fluid dynamics (CFD) and computational structural mechanics (CSM) will be used as examples of high-fidelity models for the two interacting disciplines (fluids and structures). The low-fidelity models will be represented by a nonlinear vortex-augmented panel code for the fluid model, and a 1D beam in torsion model for the wing structure. The targeted application is that of a flying wing UAV similar to a simplified X-47 UCAV configuration. In this hypothetical problem, the objective will be to achieve good



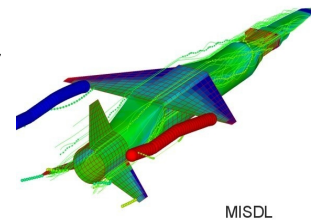
loitering properties while also being capable of rapid maneuvering. This will be modeled by designing the AUV wing planform, thickness, and deformable structure so as to minimize the drag at cruise condition, subject to lift and size constraints, while simultaneously maximizing  $C_{L,\alpha}$  for maneuverability. It is anticipated that the wing leading and trailing edges will be parameterized using Chebishev polynomials. Additional design variables include the span, root chord, and taper ratio of the wing.

The high-fidelity structural analysis tool will be McIntosh Structural Dynamics' finite element code *CNEVAL*, available in-house. *CNEVAL* (Lesieutre et al., 1997) provides the structural displacements, stresses, frequencies, and weights, and will be used to verify that structural limits are not exceeded. *CNEVAL* uses the current wing planform information, along with the planform thickness information and material properties, and updates the finite-element model of the wing which is subdivided into quadrilateral panels used to distribute the aerodynamic loads for the wing displacement calculations. The low-fidelity 1D beam-in-torsion model will be a finite element model divided into adjoining segments. The material properties of each segment will be designed to match the inertial characteristics of wing cross-sections such that the bending and torsion modes attempt to match the natural frequencies of the wing. The loads applied to each beam element will be the resulting lift and moment forces applied section by section. The high-fidelity fluid model will be NASA's *OVERFLOW* code (Buning et al. 2000) with which NEAR has considerable experience. The wing cross-sectional profile will be chosen to be specified as a parameterized family of airfoils (these parameters are, thus, additional design variables in the high-fidelity case). Automatic grid regeneration will be carried out



using either NASA's *HYPGEN* code (Chan et al., 1993) or the commercially available *GRIDGEN/POINTWISE* code through its Glyph scripting language. NEAR has expertise in both of these codes. Finally, NEAR's intermediate-level aerodynamic prediction code *MISDL* (Lesieutre et al., 1998, Dillenius et al., 1999) will be used as the

low-fidelity fluid model. *MISDL* is based on panel methods and other classical singularity methods enhanced with models for nonlinear vortical effects. The method is applicable to subsonic and supersonic flight vehicles including aircraft, UAVs, missiles, and rockets. Circular and noncircular cross section bodies are modeled by either subsonic or supersonic sources/sinks and doublets for volume and angle of attack effects, respectively. Conformal mapping techniques are used for noncircular bodies. The fin/wing sections are modeled by a horseshoe-vortex panel method for subsonic flow and by first-order constant pressure panels for supersonic flow. Up to three lifting surface sections can be modeled and nonlinear fin and body vortices are modeled. *MISDL* predicts overall aerodynamic performance coefficients and detailed aerodynamic loading distributions. The code has seen extensive use in missile aerodynamic analysis and design (see adjoining pictures), including aerodynamic shape optimization and multidisciplinary design optimization when coupled to a structural finite element model. In recent years, the code has seen use in the analysis of manned and unmanned (UAV) aircraft.



### 3.3 Phase I Statement of Work and Schedule

The tasks that will be carried out in Phase I are as follows (in rough chronological order):

- **Task 1 – Meet with Air Force sponsor.** At the start of the Phase I effort, an initial kickoff meeting is proposed to review the proposal, discuss objectives of special interest, and discuss new research findings and how they may fit with the proposed effort and proposed timetable. It is anticipated that initial discussions will be held concerning the selection of sample problems of interest to the Air Force for the application of the technology being developed. The purpose of this meeting will be to clarify NEAR's proposal as required and to discuss the suitability of the statement of work and data options.
- **Task 2 – Develop and demonstrate multifidelity metamodel construct.** As shown in Section 3.2, the global metamodel framework is well-suited to provide the foundation for an integrated hierarchical metamodel that incorporates all of the available data. Augmented with the Kennedy-Huang expected improvement function, it will provide an integrated criterion to determine both the location *and* fidelity level of subsequent searches or evaluations. The

underlying principle of dimensionality augmentation and subsequent projection onto the high-fidelity manifold was articulated in Section 3.2 in the simplifying case of two data sources. Options to generalize this approach to multiple levels of fidelity will be explored.

- **Task 3 – Develop multifidelity sequential methods based on radial basis functions.** Radial basis functions will be inserted into the MFSKO framework. To do this, two alternatives for estimating the expected improvement function and associated intervals will be considered. First, bootstrapping type intervals will be developed for radial basis functions. Second, approximate intervals based on perturbing data point values will also be investigated. In both cases, the prospects for reducing the associated computational overhead will be investigated.
- **Task 4 – Extend convergence proof from EGO to MFSKO.** The proof of convergence to the global optimum solution from Schonlau (1997) based on a finite search space will be extended to MFSKO. Conditions on the cost and error structure will be identified to satisfy the proof together with the associated region of applicability. Also, we will investigate the prospects of extension to methods based on radial basis functions and rigorous bootstrapping based and other intervals.
- **Task 5 – Apply MFSKO and extended MFSKO to flying wing UAV design problem.** Script files and C++ code will be developed to support automatic application of the developed methods. The use of these codes will be illustrated on the multiobjective aerostructural design of a UAV flying wing using at least two levels of fidelity. These will include Euler CFD and nonlinear vortex-augmented panel methods for the fluid model, and finite element CSM and 1D beam torsion models for the structure.
- **Task 6 – Support application of MFSKO and extended MFSKO to numerical test bed.** The developed computer code will also be applied to a test bed to illustrate the practical benefits and limitations of the proposed methods. Applications will include at least one problem with multiple local minima and comparison with alternative methods from the literature. Properties such as convergence to local and global minima will be included in the study.
- **Task 7 – Investigate relationships with alternative models, fidelity levels, and model parameters.** Preliminary models for the numbers of estimated parameters and bounds on the computational efficiency for alternative methods will be developed in the context of multifidelity optimization. At least three methods will be included in the comparison: MFSKO, extended MFSKO, and trust region-based multifidelity optimization methods.
- **Task 8 – Implement gappy POD.** Time permitting, NEAR will implement the gappy Proper Orthogonal Decomposition method developed by Everson and Sirovich (1995) as an enhancement to the integrated hierarchical metamodel developed in Tasks 2-5. This method is one of several proposed by Robinson et al. (2006a,b) to deal with the case of variable fidelity models which operate on different sets of design variables. This should be a relatively straightforward task that will provide additional robustness for a foundational multifidelity computing environment.
- **Task 9 – Report.** Reporting during the course of the project will consist of bimonthly progress reports and a comprehensive final technical report. Writing the final report will involve collaboration between all senior members of the project team with limited assistance from the supported graduate student. The student will document his or her results in a graduate thesis which will not include research not permitted as part of the sponsored research agreement.

Tasks 3, 4, 6, and 7 will be performed at OSU. Tasks 2, 5, 8 and 9 will be carried out at NEAR, with OSU participation on Tasks 5 and 9.

#### Milestone Schedule

The proposed Phase I effort will be accomplished within the required nine-month period, with the majority of the primary research accomplished within the first six months of the contract. A milestone chart for each of the components defined above is shown below.

Nielsen Engineering & Research, Inc. – DoD STTR Topic Number AF08-BT03 – Proposal F08B-T03-0043  
 “Development of Multidisciplinary, Multifidelity Analysis and Integration of Aerospace Vehicles”

<b>Months After Contract Award:</b>		<b>1</b>	<b>2</b>	<b>3</b>	<b>4</b>	<b>5</b>	<b>6</b>	<b>7</b>	<b>8</b>	<b>9</b>
<i>Phase I:</i>										
1	Meet with Air Force sponsor	X								
2	Multifidelity Meta Model Construct		X				X			
3	Multifidelity Sequential RBF		X							
4	MFSKO Convergence Proof			X						
5	Application to UAV Design					X				
6	Numerical Test Bed					X				
7	Alternative Models									
8	Gappy P.O.D. Mapping								X	
9	Reporting		X		X		X		X	X